Received: 17 April 2020 | Revised: 31 August 2020 | Accepted: 27 September 2020

DOI: 10.1002/2050-7038.12674

RESEARCH ARTICLE

WILEY

A novel fuzzy tuned multistage PID approach for frequency dynamics control in an islanded microgrid

Anil Annamraju | **Srikanth Nandiraju**

Department of Electrical Engineering, National Institute of Technology Warangal, Hanamkonda, India

Correspondence
Anil Annamraju, Department of Electrical Engineering, National Institute of Technology Warangal, Hanamkonda, Telangana, India.
Email: aakumar@student.nitw.ac.in

Handling Editor: M. Hadi Amini

Abstract

Objective: In microgrid (MG), besides the load perturbation, volatile nature in renewable output power along with energy storage system and inertia uncertainties cause large frequency deviations which may weaken the MG and could lead to complete blackout. Therefore, MG requires an intelligent, efficient and robust control method.

Methods: In response to this challenge, this paper proposes a novel fuzzy logic approach (FLA) tuned multistage PID controller for frequency control of an islanded MG in the presence of high renewable penetration. The proposed controller is intended for principal parameter tuning of multistage PID controller under critical operating conditions as mentioned in the objective.

Results: The real-time MG test system is considered to present the simulation results. The test system is modelled in Matlab/Simulink. The results are carried out under different operating scenarios and the performances of the proposed technique are compared with various existing techniques in the literature.

Conclusions: The simulation outcomes divulge that the proposed controller is more superior in improving the frequency dynamics of the MG (in terms of settling time, overshoot and error reduction) under various disturbance conditions. Furthermore, the proposed controller is more robust to renewable and energy storage system uncertainties in MG and less sensitive to MG parametric variations as compared to other controllers in literature.

List of symbols and abbreviations: BESS, Battery Energy Storage System; DEG, Diesel Engine Generator; ESS, Energy Storage Systems; FC, Fuel Cell; FESS, Flywheel Energy Storage System; FLA, Fuzzy Logic Approach; GOA, Grasshopper Optimization Algorithm; ITAE, Integral Time Multiplied Absolute Error; LFC, Load Frequency Control; LN, Large Negative; LP, Large Positive; MFs, Membership Functions; MG, Microgrid; MN, Medium Negative; MP, Medium Positive; PID, Proportional Integral Derivative; PD, Proportional Derivative; PI, Proportional Integral; PV, Photovoltaic; RES, Renewable Energy Sources; STC, Standard Temperature Condition; TF, Transfer function; WTG, Wind Turbine Generator; Z, Zero; M, Moment of inertia; D, Damping coefficient; R, Speed regulation constant; Δf, Frequency deviation; Δf^*, Change in Frequency deviation; K_{BESS}, K_{FESS}, Gains of BESS and FESS; K_{FC}, Gain of FC; K_{PV}, K_{WTG}, Gains of PV array, WTG; T_{BESS},T_{FESS}, Time constant of BESS,FESS; T_{FC}, Time constant of FC; T_1, Time constant of the governor; T_2, Time constant of transport delay; T_3, Time constant of diesel generator; T_{PV}, T_{WTG}, Time constant of PV and WTG models; ΔP_{DEG}, Change in DEG output power; ΔP_L, Change in load; ΔP_{BESS}, Change in BESS Power; ΔP_{FESS}, Change in FESS Power; ΔP_{FC}, Change in FC power; ΔP_{WTG}, Change in WTG output power; ΔP_{PV}, Change in solar power; ΔP_{WP}, Change in mechanical wind power; ΔP_{φ}, Change in solar radiation; P_{solar}, Rated output power of PV array; P_{wp}, Mechanical wind power output; Φ, Irradiation; φ_{STC}, Irradiation at a standard temperature condition; K_e, K_{ce}, Scaling factor of MFs of fuzzy inputs; K_{u1}, K_{u2}, K_{u3}, K_{u4}, Scaling factor of MFs of fuzzy outputs; U_{c1}, U_{c2}, U_{c3}, U_{c4}, Fuzzy outputs; ΔK_P, Change in a proportional gain in PD stage; ΔK_{PP}, Change in a proportional gain in PI stage; ΔK_I, Change in an Integral gain; ΔK_D, Change in a derivative gain; T_s, Settling time; U_f, Control signal from the controller; V_{cut-in}, Cut-in wind velocity of WTG; $V_{cut-out}$, Cut-out wind velocity of WTG; V_{rated}, Rated wind velocity; C_P, Power coefficient; ρ, Air density; A, Swept Area; λ, Tip speed ratio; β, Pitch angle; R, Radius of blade; ω, Angular velocity; T_a, Ambient Temperature; T_{STC}, Temperature at STC.

KEYWORDS

energy storage system uncertainties, frequency control, fuzzy logic approach, microgrid, multistage PID controller

1 | INTRODUCTION

In the present power system scenario, microgrid (MG) helps in supplying electrical energy to remote places and island locations where the electrical energy from the main grid is too costly, complicated, and environmentally hazardous. For such conditions, an MG would be an efficient and reliable solution.[1] An MG can be operated in two modes, viz, islanded mode and grid-connected mode. The intermittent nature of RES along with low system inertia of diesel engine generators (DEGs) makes islanded mode of operation complicated than the grid-connected mode.[2] Whereas in grid-connected mode, the initial frequency support is adjusted by the main power system network. Therefore, if any generation-load imbalance creates large frequency deviations in an islanded MG, which leads to degradation power system operation and reliability, sometimes may lead to MG blackout.[3] For such conditions, load-frequency control (LFC) is of utmost importance. It operates constantly to maintain a balance between the load demand and the power generation and tries to restore the frequency to the rated value.[4]

1.1 | Motivation

In conventional power systems, the LFC task is quite simple because the disturbances are arising from the load side only. Where, in MG, diversity in generation/load, functional complexity, change of structure (uncertainty), and variable nature of RES are some key intrinsic characteristics, which make the frequency control quite complex.[5] The conventional and optimal controllers fail to provide acceptable performance under these circumstances due to its fixed gains of the system based on predetermined operating conditions.[6] Therefore, due to rapid change in operating conditions, these controllers may not provide satisfactory performance in some critical operating scenarios. By accounting the above factors, frequency control of MG in an islanded operation requires an efficient and intelligent controller.[7] This paper aims to provide an efficient frequency control strategy for an autonomous microgrid in secondary frequency control loops.

1.2 | Related works and key gaps

The MG has two structures in secondary frequency control, which are centralized structure and decentralized structure. For grid-connected mode, the decentralized structure is preferred, whereas for an islanded microgrid, centralized structure is preferred.[8] With the centralized structure, several authors proposed various control strategies for LFC of MG.[9-30] Serban and Marinescu[9] proposed Ziegler-Nicholas tuned PI controller for LFC of an autonomous MG, where the gains of the PI controller are tuned by Ziegler-Nicholas approach. Yang et al[10,11] proposed an optimal PI/PID controller for MG frequency control. Khalghani et al[12] proposed self-tuning PID controller, Grover et al[13] proposed adaptive control method, Jeya Veronica and Senthil Kumar[14] proposed internal model control (IMC) method, Pahasa and Ngamroo[15] proposed model predictive control method, Shedom et al[16] proposed H-∞ control based robust controller, Shashi and Soumya[17] proposed LMI based robust control approach, and Mi et al[18] proposed sliding mode control (SMC) for frequency control of an islanded MG.

However, in practical industrial applications, the PID controller is used mostly due to its reliability, good performance, and simple structure with acceptable cost. To meet the operational challenges in MG frequency control, several authors proposed various intelligent techniques to optimize the PID controller parameters according to MG operating conditions. In,[19-28] the authors proposed various swarm-intelligence methods for LFC of MG. Das et al[19] proposed genetic algorithm (GA) based PID controller, Srinivasarathnam et al[20] proposed grey wolf optimization (GWO) based PID controller, El-Fergany and El-Hameed[21] proposed social spider optimization (SSO) based PID controller, Shankar and Mukherjee[22] proposed harmony search algorithm based PID controller, Ray and Mohanty[23] proposed firefly algorithm based PID controller, and Shankar et al[24] proposed fruit fly algorithm-based PID controller for LFC of MG. However, most of the performance of the swarm-intelligence techniques relies on their algorithm-specific parameters, and improper selection of these parameters may lead the solution toward the local minima.[25] For further

improvements in frequency control, several authors proposed neural network-based schemes in MG frequency control.[26,27] Bevrani et al[26] proposed a generalized artificial neural network (ANN) based model for LFC of an MG. Safari et al.[27] proposed PSO optimized ANN controller for LFC of an MG. However, a general limitation with these techniques is that it operates the system as a black box and analyzes it functionally. Moreover, for each problem, it has to be trained separately, and a large number of tests are performed to define the adequate algorithm architecture. To overcome these problems, several authors proposed fuzzy logic approach (FLA) based schemes for optimizing PI/PID controllers for frequency control of MG.[28,29] Khezri et al[28] proposed a robust fuzzy PI controller, where the parameters of PI controller are optimized with the FLA to obtain robust performance in frequency control. Bevrani et al,[29] proposed an FLC for MG frequency control under diverse operating conditions. From the literature survey, the FLA is proven as an efficient solution for various problems encountered in MG. Moreover, the FLA approach can handle system nonlinearities and uncertainties in a better manner even though for continuous change in the system structure. On the other hand, the limitation of using a classical PID controller is that it is ambitious to find its optimal state. This is only due to the trade-off between the derivative and integral part. The steady-state error is minimized by the use of the PI controller. The increase in an integral part solves the above limitation but an undesired behavior is observed during the transient state due to extra integral term in the controller. In the transient state, the presence of an integral term increases the feedback error by increasing the corrective response, which essentially reduces the stability and speed of the system. Furthermore, to realize the best performance of PID controller design, trade-off between derivative and integral gain has become a challenge. To minimize steady-state error, the integral part should increase, thus there is an inclusion of integral term during the transient state, but the integral term should be present only during steady-state. This limitation can be eliminated by the use of a multistage PID controller.[30]

1.3 | Contributions

In this work, the combination of FLA and multistage PID controller is used to design a novel robust controller for LFC of an islanded MG. Till now, no one has addressed the tuning of multistage PID controller with FLA. To obtain the inherent merits of both the controllers, in this work, the FLA is utilized to tune the parameters of the multistage PID controller. In the proposed work, instead of gain scheduling, the gains of controllers are tuned according to operating conditions. From the literature, to design an efficient LFC controller for modern power systems, the following specifications have to be met:

S_1 : Efficient against load disturbances
S_2 : Robust against RES uncertainties
S_3 : Less sensitive to MG uncertainties
S_4 : Constructive and effective in handling ESS uncertainties
S_5 : Adaptable and flexible in tuning according to system operating conditions.

To meet all these specifications, the MG is subjected to various operating scenarios, and performance of the MG is analyzed with the proposed controller. Moreover, the performance of the proposed controller is evaluated by comparing with various powerful techniques published in the literature.

The key contributions of this paper are:

1. A novel fuzzy tuned multistage PID controller is proposed for LFC analysis of an islanded MG, and its performance is compared with other popular techniques in the literature like GOA PID, Fuzzy PID, and multistage PID controllers.
2. A first attempt has been made to optimize the parameters of the multistage PID controller with FLA.
3. The robustness of the proposed controller is tested against RES uncertainties, MG uncertainties, and energy storage system uncertainties with diverse operating scenarios in a single controller framework.
4. An attempt has been made to meet all the possible specifications of a good LFC as stated in the literature simultaneously.

1.4 | Organization of the paper

Figure 1 depicts the schematic overview of this research work. The rest of the paper is organized as follows: Section 2 depicts the mathematical modeling of MG test system, Section 3 illustrates the proposed fuzzy tuned multistage PID

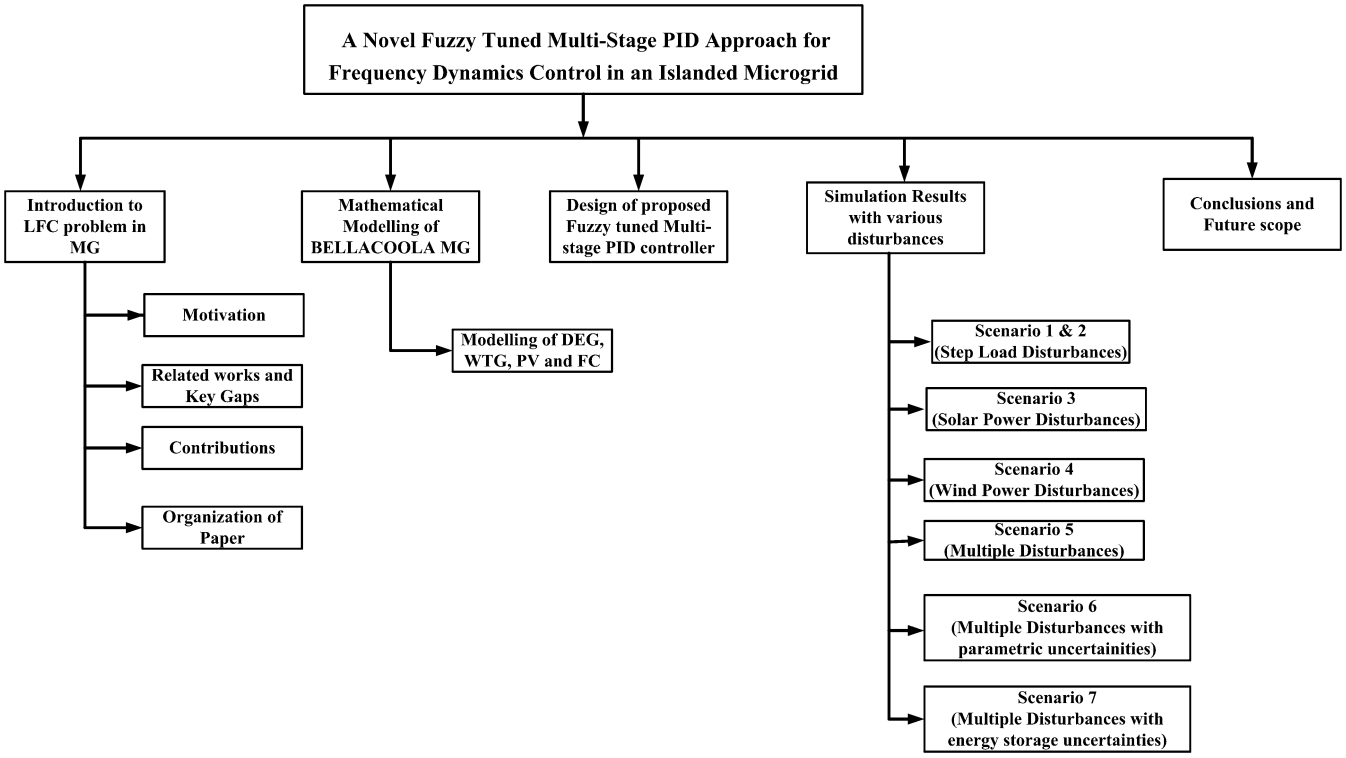

FIGURE 1 Schematic overview of the paper

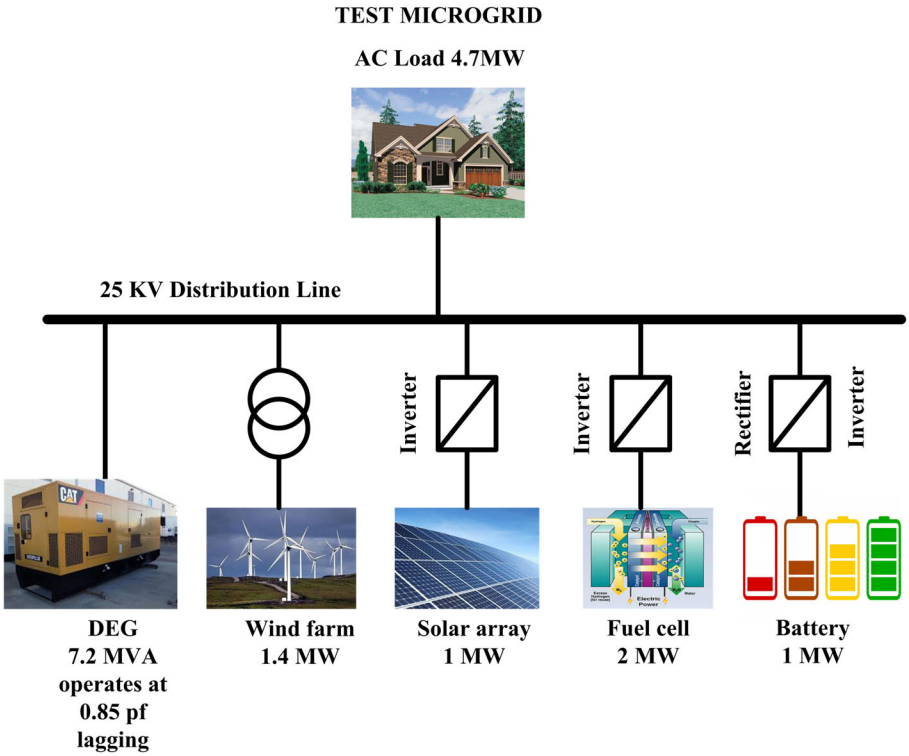

FIGURE 2 Schematic model of the test system

controller, Section 4 demonstrates the frequency response of MG with various controllers subjected to different operating scenarios, Section 5 deomonstrates the observations from simulation results and finally Section 6 concludes the overall outcomes in the proposed work.

2 | MATHEMATICAL MODELING OF THE INVESTIGATED HYBRID MICROGRID

Figure 2 depicts the schematic model of MG test system with various energy sources.[31] The simplified mathematical model of the test system under investigation is shown in Figure 3. This system consists of a DEG and fuel cell (FC) with a control mechanism, load model, the real-time WTG and PV models, and various primary ESSs like FESS and BESS (In Fig.2 BESS and FESS together shown as Battery).

A comprehensive explanation with regards to each MG component is discussed in the subsequent sections. The simulation parameters of MG are listed in Table 1.[32]

From Figure 3, the MG output power balance equation can be expressed as follows:

$$\Delta P_{WTG} + \Delta P_{PV} \pm \Delta P_{BESS} + \Delta P_{DEG} + \Delta P_{FC} \pm \Delta P_{FESS} = \Delta P_{LOAD}. \quad (1)$$

In MG, the change in frequency deviation due to load and RES output power changes can be expressed as follows:

$$\Delta f = \frac{1}{Ms + D}(\Delta P_{DEG} + \Delta P_{WTG} + \Delta P_{PV} + \Delta P_{FC} - \Delta P_{BESS} - \Delta P_{FESS} - \beta\Delta f - \Delta P_L). \quad (2)$$

The objective of the controller is to minimize the frequency deviations to a minimum value (ideally zero) by meeting the specifications (S_1-S_5) as mentioned in the literature. In the proposed work, DEG and FC will take care of generation-load balance with the help of the proposed controller.

2.1 | DEGs

Due to the inherent features of DEG, including high efficiency, low maintenance, and fast starting speed, it is a very good backup option in autonomous MGs. The properly controlled DEG can quickly track the load changes through its

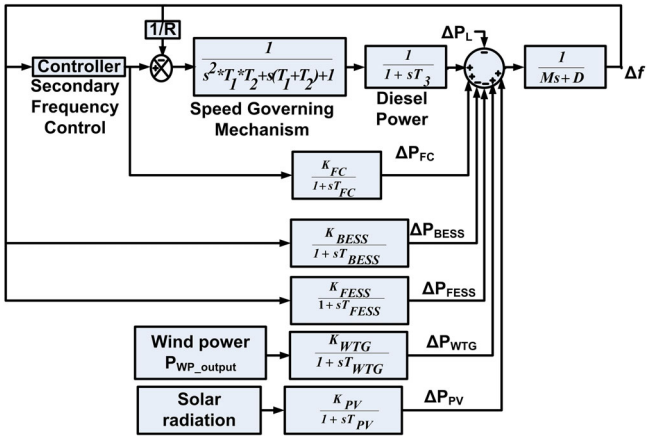

FIGURE 3 Mathematical Model of investigated MG

TABLE 1 Simulation parameters of microgrid (MG)

Parameter	Value	Parameter	Value
$M(s)$	0.1667	T_2(s)	2
$D(puMW)$	0.015	$T_3(s)$	3
K_{BESS}	1.5	T_{BESS} , T_{FESS}(s)	0.1
K_{WTG}	1	T_{FC} (s)	4
K_{PV}	1	T_{PV} (s)	1.5
$T_1(s)$	0.025	T_{WTG} (s)	2

power control mechanism. Moreover, the fluctuation of uncontrollable RES and loads can be effectively compensated by the DEGs.

DEG can be represented by a combination of speed governor and diesel engine, as shown in Figure 4. In Figure 4, U_f and Δf represent the LFC control signal for DEG and frequency deviation of MG, respectively. Based on this signal, the governor adjusts the valve position (ΔX) to accommodate the load changes (ΔP_L).

2.2 | Wind turbine generator (WTG)

Due to the volatile nature of wind speed, the WTG output power changes nonlinearly according to wind speed and the wind directions. In connection to MPPT limitation and intermittency in RES output power, these RES are not considered in LFC. In this work, only DEG and FCs can take care of LFC duties. Therefore, the WTG can be modeled as a disturbance and an uncontrolled power source in LFC analysis. Figure 5 shows the mathematical model for the random wind velocity generation pattern.

In general, the windmill output power can be expressed as follows:

$$P_{wp} = 0.5\rho A V_w^3 C_p(\beta,\lambda) \tag{3}$$

where "V_w" is the wind velocity, "ρ" is the air density, "A" is the swept area, and C_p is power coefficient, which is a function of tip speed ratio (λ), pitch angle (β), and it can be expressed as follows[33]:

$$C_p(\beta,\lambda) = \left(\frac{25.52}{\gamma} - 1.1 - 0.088\beta\right) * exp^{-125/\gamma}, \tag{4}$$

$$\gamma = 1/\left[\frac{1}{\lambda + 0.08\beta} - \frac{0.035}{1+\beta^3}\right]$$

$$\lambda = \frac{R\omega}{V_w},$$

where "R" is the radius of the blade and "ω" is the angular velocity of the induction generator. In the present work, GAMESA Company manufactured WTG data are utilized for LFC analysis, and the details and ratings of WTG are given in Table A2. Based on windmill output power (P_{wp}) at different wind speeds (V_W), an equation for P_{wp} is developed in terms of V_W.[21]

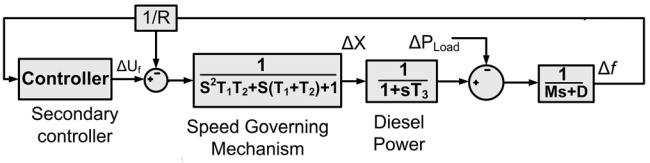

FIGURE 4 Mathematical model of diesel engine generator (DEG)

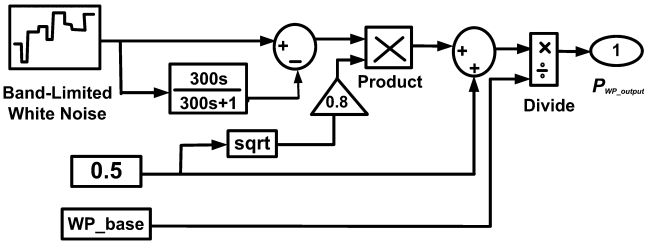

FIGURE 5 Block diagram model for wind velocity pattern generation

$$P_{wm}=\begin{cases}0.0013V_w^6-0.046V_w^5+0.33V_w^4+3.68V_w^3-51V_w^2+2.33V_w+366, V_{cutin}\le V_w\le V_{rated}\\ P_{rated}, V_{rated}\le V_w\le V_{cutout}\\ 0, > V_{cutout}\end{cases}. \quad (5)$$

LFC analysis is related to the small-signal stability analysis, hence change in "P_{wp}" is needed. It can be obtained by differentiating Equation (5), which is expressed as follows:

$$\Delta P_{wp}=\begin{cases}\left(0.0078V_w^5-0.23V_w^4+1.32V_w^3+11.04V_w^2-102V_w+2.33\right)*\Delta V_w, V_{cutin}\le V_w\le V_{rated}0,\\ V_{rated}\le V_w\le V_{cutout}\\ 0, > V_{cutout}\end{cases}. \quad (6)$$

The transfer function model of the WTG system can be expressed as follows:

$$TF_{WTG}=\frac{\Delta P_{WTG}}{\Delta P_{wp}}=\frac{K_{WTG}}{1+sT_{WTG}}. \quad (7)$$

2.3 | PV array

The PV array is the combination of modules in parallel and series, and this combination relies on the desired current and voltage ratings of the MG. The output power of the PV array is volatile by nature and it depends on solar irradiation and temperature. The output power of the PV array (P_{PV}) can be expressed as follows[34]:

$$P_{PV}=P_{solar}*\frac{\varphi}{\varphi_{STC}}*\left(1+K_t*\left[T_a+0.0256*\varphi*\Delta\varphi-T_{STC}\right]\right) \quad (8)$$

ΔP_{PV} based on the change in irradiation can be computed using Equation (9):

$$\Delta P_{PV}=\frac{P_{solar}}{\varphi_{STC}}*\left(\Delta\varphi+K_t\left[\Delta\varphi*T_a+\varphi*\Delta T_a+0.0512*\varphi*\Delta\varphi-T_{STC}*\Delta\varphi\right]\right). \quad (9)$$

The first-order model of the PV system can be expressed as follows[34]:

$$TF_{PV}=\frac{\Delta P_{PV}}{\Delta\varphi}=\frac{K_{PV}}{1+sT_{PV}} \quad (10)$$

K_{PV} denotes the gain of the PV array and T_{PV} indicates the time constant of PV array, including converter time delay also. The ratings of PV array is available in Table A3.

2.4 | Fuel cells

Conventional LFC regulating units like DEGs are quite sluggish for short-term frequency deviations due to lethargic time constants involved in DEGs. The unanticipated changes in PV and wind output powers cause short-term transients in frequency deviations of MG. To conquer these problems, the ESSs have turned a vital part in LFC of MG and one of the most promising ESS to meet the LFC requirements are FCs. The FCs offer several attracting features, such as full discharging capabilities, low cost, high energy efficiencies, and relatively easy to maintain compared to other ESSs.[35] The transfer function model of FCs for LFC studies can be expressed as follows:

$$TF_{FC} = \frac{\Delta P_{FC}}{U_f} = \frac{K_{FC}}{1 + sT_{FC}}. \tag{11}$$

3 | PROPOSED FUZZY TUNED MULTISTAGE PID CONTROLLER DESIGN

The proposed controller comprises of two stages. One is multistage PID controller and the second one is FLA. A detailed explanation of each stage is explained in the subsequent sections.

3.1 | Multistage PID controller

Multistage PID (Proportional Integral and Derivative) controller is the series combination of PD and PI controllers. This controller comprises of PD controller in its first stage and PI controller in the second stage. Error (Δf) is the input to the first stage, which is PD controller. The output of the PD part is considered as the input to the PI part. The final controller output is "U_f," which is the output of the PI controller. To change the controllable sources (DEGs and FCs), reference power setting is used as the controller output (U_f). The process can be controlled and better performance can be achieved by the use of three parameters.

The mathematical equation for the classical PID controller can be expressed as follows[5]:

$$U_f = \left(K_P + K_D * s + \frac{K_I}{s}\right) * \Delta f. \tag{12}$$

In multistage PID controller, the best features of both controllers—PD and PI controllers—can be used. In the PI controller, the integral term should be present during steady-state and the output is constant to the PD controller. It means that integral output will be zero during transient, which avoids the limitation of classical PID. This controller has been successfully applied to various engineering problems. The multistage PID controller can be executed as shown in Figure 6.

The mathematical model for multistage PID controller can be expressed as follows[30]:

$$U_f = (K_P + K_D * s)\left(1 + K_{PP} + \frac{K_I}{s}\right) * \Delta f. \tag{13}$$

3.2 | Fuzzy tuned multistage PID controller

Figure 7 shows the structure of the proposed fuzzy tuned multistage PID controller. In the proposed controller, the parameters of the multistage PID controller are tuned with FLA. The detailed information of FLA is available in the literature.[36,37] The FLA mainly consists of three blocks, viz, fuzzification, inference engine, and defuzzification. Here, Mamdani type FLA is employed. In the fuzzification process, the inputs (Δf, Δf^*) and outputs of FLA (ΔK_P, ΔK_D, ΔK_{PP}, ΔK_I) are converted into fuzzified variables using five normalized membership functions (MFs), namely LN, MN, Z, MP, and LP. The MFs for inputs and outputs are shown in Figure 8. Here, triangular MFs are used due to their adaptability and simplicity in the inference process.

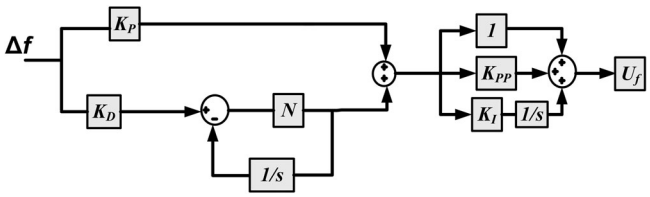

FIGURE 6 Structure of multistage PID controller

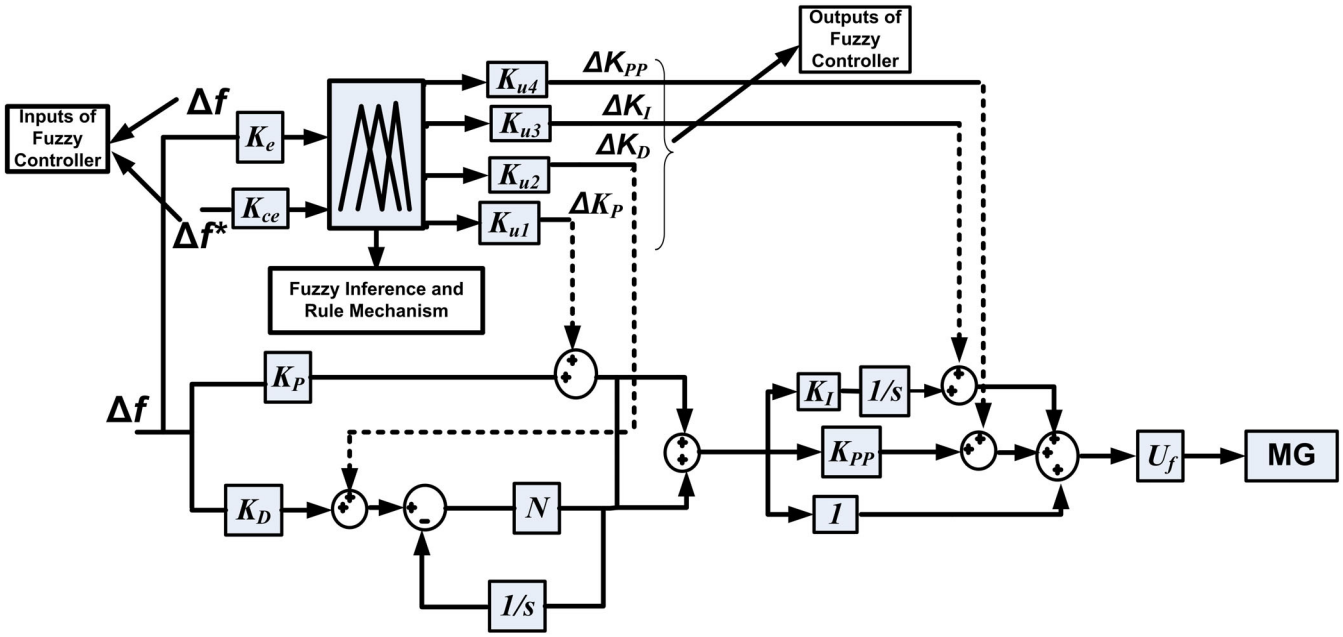

FIGURE 7 Structure of proposed fuzzy-tuned multistage PID controller approach

FIGURE 8 Membership functions (MFs) for inputs and outputs of fuzzy logic approach (FLA)

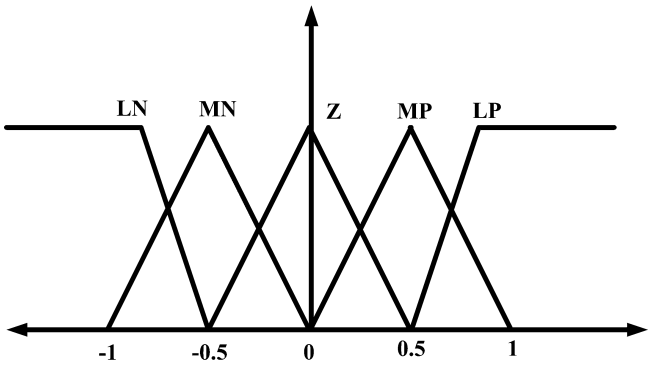

The second part of FLA is the inference engine, which consists of a fuzzy rule base and information about the linguistic variables for required control action. A lookup table is set up to determine the appropriate control action based on all possible combinations of input variables. The rule base, which maps the inputs and outputs of FLA, is given in Tables 2-4. There are a total of five membership functions in inputs and outputs of FLA. Therefore, a total of 25 rules were framed to implement the proposed multistage PID controller for perturbing MG. For example, the 15th rule in rule base of FLA (from Tables 2-4) can be expressed as follows:

Rule 15: If frequency deviation (**Δf**) is Z and the change in frequency deviation (**Δf***) is LP then change in (**ΔK_P** & **ΔK_{PP}**) is LN and change in (**ΔK_I**) is LP and (**ΔK_D**) is Z.

Likewise, in the given simulation time, based on Δf and Δf* conditions with the inference of 25 rules and deciding factor of each fired rule, overall ΔK_P, ΔK_{PP}, ΔK_I, and ΔK_D values are estimated by fuzzy defuzzification. Based on that, the values of K_P, K_{PP}, K_I, and K_D values are adjusted according to Equation (19).

The last and final stage in FLA is defuzzification. In this stage, the aggregated fuzzy singleton outputs are converted to an equivalent crisp value, which is the required output of FLA. The centroid method of defuzzification is used in this work. The output of FLA can be expressed as follows[38]:

TABLE 2 Fuzzy logic approach (FLA) rule base for ΔK_P and ΔK_{PP}

	Δf^*				
Δf	LN	MN	Z	MP	LP
LN	LP	LP	LP	MP	Z
ML	LP	LP	MP	Z	MN
Z	LP	MP	Z	MN	LN
MP	MP	Z	MN	LN	LN
LP	Z	MN	LN	LN	LN

TABLE 3 FLA rule base for ΔK_I

	Δf^*				
Δf	LN	MN	Z	MP	LP
LN	LN	LN	LN	NM	Z
ML	LN	LN	MN	Z	MP
Z	LN	MN	Z	MP	LP
MP	MN	Z	MP	LP	LP
LP	Z	PM	LP	LP	LP

TABLE 4 FLA rule base for ΔK_D

	Δf^*				
Δf	LN	MN	Z	MP	LP
LN	MP	MN	LN	LN	MP
ML	MP	MN	MN	MN	Z
Z	Z	MN	MN	MN	Z
MP	Z	MP	MP	MP	LP
LP	LP	LP	MP	MP	LP

$$U_{c1}, U_{c2}, U_{c3}, U_{c4} = \frac{\sum_{j=1}^{f} A_i Q_l}{\sum_{j=1}^{f} Q_l}, \tag{14}$$

where A_i represents the total firing area of j rules, 'f 'represents the total number of partitions of the fired area, and Q_l represents the center of an area.

From the fuzzy outputs, the change in gains of the multistage PID controller can be written as follows:

$$\Delta K_P = K_{u1} \mathrm{U_{c1}} \tag{15}$$

$$\Delta K_D = K_{u2} \mathrm{U_{c2}} \tag{16}$$

$$\Delta K_I = K_{u3} \mathrm{U_{c3}} \tag{17}$$

$$\Delta K_{PP} = K_{u4} \mathrm{U_{c4}}, \tag{18}$$

where K_{u1}, K_{u2}, K_{u3}, and K_{u4} are the scaling factors of FLA output variables. Where K_e and K_{ce} denotes the scaling factors of input variables. From Equations (15)-(17), the expression for control action by fuzzy tuned multistage PID controller can be expressed as follows:

$$U_f = ([K_P + \Delta K_P] + [K_D + \Delta K_D] * s) * \left[1 + (K_{PP} + \Delta K_{PP}) + \frac{(K_I + \Delta K_I)}{s}\right], \tag{19}$$

where "U_f" is the control action fed to DEG and FC for frequency control according to power changes.

4 | RESULTS AND DISCUSSION

In this section, to examine the proposed controller, LFC analysis on Practical MG test system has been performed under different operating scenarios.[39] The test system shown in Figure 3 is simulated in MATLAB 2015 software. Simulation parameters of the test system are given in Table 1. In this work, to show the effectiveness of the multistage PID controller over normal PID controller, both controller parameters are optimized by using a recently developed grasshopper optimization algorithm (GOA). The detailed information about GOA to LFC problem is available in.[5,40] Thereafter, the performance of the proposed fuzzy tuned multistage PID controller is compared with that of GOA tuned multistage PID controller, GOA tuned PID controller, and Fuzzy tuned PID controller. To assess the performance of the proposed controller, the test system is subjected to various disturbances like load, RES output power variations, and various uncertainties in MG and ESSs. To exhibit the superiority of the proposed controller, time-domain simulations of the proposed controller and other controllers are compared case by case in each scenario.

4.1 | Scenario 1: performance evaluation of various controllers against step load disturbances

In this scenario, the load in MG is increased suddenly by 10% and the respective frequency response of MG with various controllers is depicted in Figure 9. It has been observed that the increase in load demand causes a decrease in frequency deviation; due to controller action, the frequency deviations attained steady-state value after some time. The quantitative analysis of Figure 9 in terms of overshoots/undershoots and settling times are given in Table 5. The heuristic gains of the PID controller with various swarm-intelligence methods are given in Table 6.

The objective of the GOA optimized PID and multistage PID controller is to minimize the frequency deviations in MG. To achieve this, integral time multiplied absolute error (ITAE) criteria is selected as the fitness function. There are a variety of error functions available in the control system like integral absolute error (IAE) and integral square error (ISE). Among them, an ITAE criterion is most popular and suitable for frequency control studies.[7] The ITAE criteria can be expressed as follows:

$$\text{ITAE} = \text{minimization of} \int_0^{t_{sim}} t * |\Delta f| dt. \tag{20}$$

Subjected to the optimization of $0 \leq K_P, K_{PP}, K_I, K_D \leq 5$. Where "$t_{sim}$" denotes the total simulation time and "t" denotes the sample at which frequency error is considered.

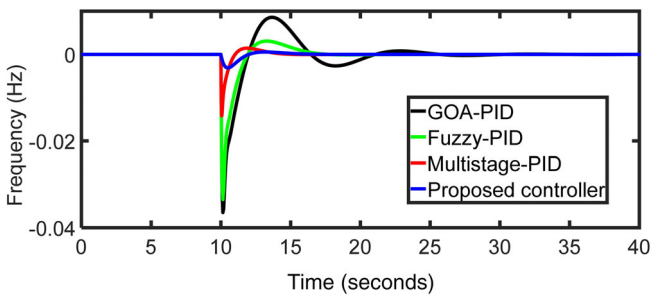

FIGURE 9 Frequency response of microgrid (MG) against step load disturbance

TABLE 5 Dynamic response analysis of various controllers for scenario-1 conditions

Methods	Performance indices			
	PUS (Hz)	POS (Hz)	T_s (s)	ITAE
GOA-PID	−0.038	0.025	17	0.000023
Fuzzy-PID	−0.035	0.006	11	0.000017
GOA-multistage PID	−0.018	0.0028	7	0.0000048
Proposed controller	−0.005	0	4	0.0000016

TABLE 6 Optimized gains of various controllers

Methods	Optimized gains			
	K_P	K_I	K_{PP}	K_D
GOA-PID	2.45	1.36	-	2.36
Fuzzy-PID	4.4152	0.4545	-	2.5862
GOA-multistage PID	2.49	1.36	2.2	2.36
Proposed controller	4.4152	0.4542	1.1	1.138

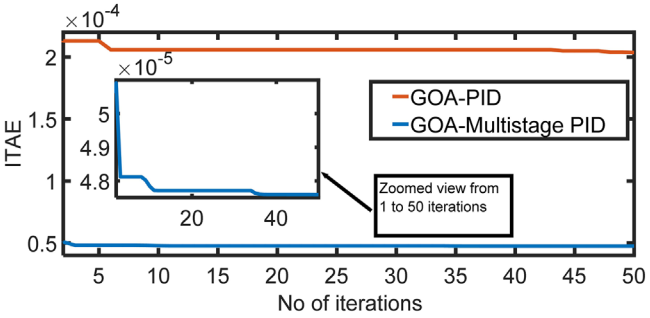

FIGURE 10 ITAE performance of GOA-PID and GOA-multistage PID controllers

The objective of the fitness function is to minimize the magnitude of frequency deviations in iteration to iteration. From Figure 10, it is clear that, compared to GOA-PID controller, GOA multistage PID controller obtained a low ITAE value from the initial iteration itself. This is due to the effective utilization of PID controller in multistage where an optimal tradeoff between I and D controllers has been obtained. Thus, GOA-multistage PID controller obtains a better frequency response over GOA-PID controller. Furthermore, with the proposed fuzzy tuned multistage PID controller, the frequency response of MG has been improved significantly over GOA-multistage PID controller.

4.2 | Scenario 2: performance evaluation of various controllers against multi-step load disturbances

In this scenario, the load in MG is increased and decreased randomly at different time intervals as shown in Figure 11A. The MG frequency responses with various controllers at different time intervals are depicted in Figure 11B. The quantitative analysis of Figure 11B in terms of overshoots/undershoots and settling times are given in Table 7.

4.3 | Scenario 3: performance evaluation of various controllers against solar power disturbances (ΔP_{PV})

In this scenario, only ΔP_{PV} is considered in MG as shown in Figure 12A. The frequency response of MG is depicted in Figure 12B,C. For a better view of results, in Figure 12B, three controllers are compared and the best controller among the three (ie, GOA-multistage PID controller) is compared with the proposed controller shown in Figure 12C.

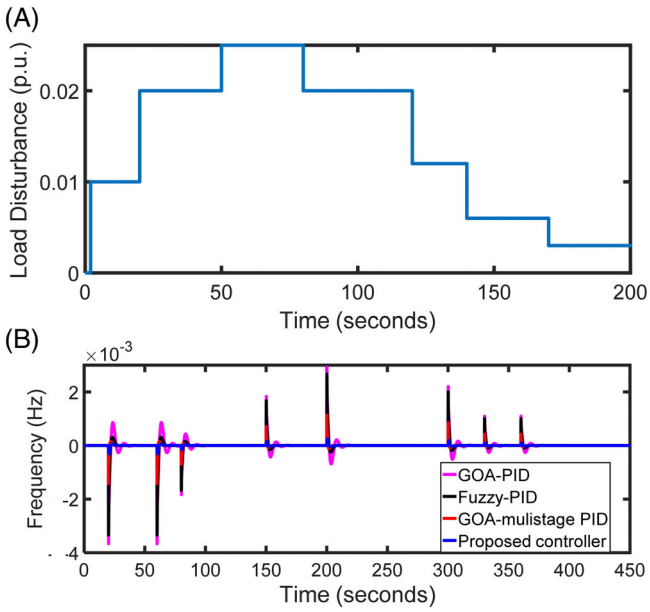

FIGURE 11 A, Multi-step load disturbances. B, Frequency response of MG against multi-step load disturbance

TABLE 7 Dynamic response analysis of various controllers for scenario-1 conditions

Disturbance at various instances	GOA-PID			Fuzzy-PID			GOA multistage			Proposed controller		
	PUS	POS	T_s	PUS	POS	T_s	PUS	POS	T_s	PUS	POS	T_s
At t = 20 s	−0.0035	0.0009	18	−0.0023	0.0003	12	−0.0014	0.0001	7	−0.0003	0.00005	4
At t = 60 s	−0.0038	0.001	20	−0.0031	0.0003	10	−0.0015	0.00015	8	−0.0004	0.00006	5
At t = 80 s	−0.0005	0.0018	17	−0.0017	0.0002	9	−0.0007	0	7	−0.0002	0	4
At t = 150 s	−0.0005	0.0019	12	−0.0002	0.0016	10	−0.0001	0.0007	7	0	0.0002	5
At t = 200 s	−0.0028	0.001	16	−0.0003	0.0025	11	−0.0002	0.0009	6	0	0.0001	4
At t = 300 s	−0.0006	0.0022	18	−0.0002	0.002	9	−0.0001	0.0008	6	0	0.0002	4
At t = 330 s	−0.0003	0.0001	11	−0.0001	0.001	8	0	0.0004	6	0	0.0011	4
At t = 360 s	−0.0003	0.0001	13	−0.0001	0.001	8	0	0.0094	6	0	0.001	4
ITAE	0.0029049			0.0097365			0.00168			0.000596		

4.4 | Scenario 4: performance evaluation of various controllers against wind power disturbances

In this scenario, only wind power disturbances (ΔP_{WTG}) are considered in MG as shown in Figure 13A. The MG frequency response is depicted in Figure 13B,C.

4.5 | Scenario 5: performance evaluation of various controllers against multiple disturbances

In this scenario, all the possible disturbances in MG (ie, ΔP_L, ΔP_{WTG}, and ΔP_{PV}) are considered simultaneously as shown in Figure 14A. The MG frequency response is depicted in Figure 14B,C.

From Figure 14B,C, it can be noticed that the MG experiences better frequency response with proposed controller as compared to other controllers in the literature. The performance evaluation of various controllers in terms of various specifications like PUS/POS and ITAE is depicted in Table 8. From quantitative analysis, the proposed

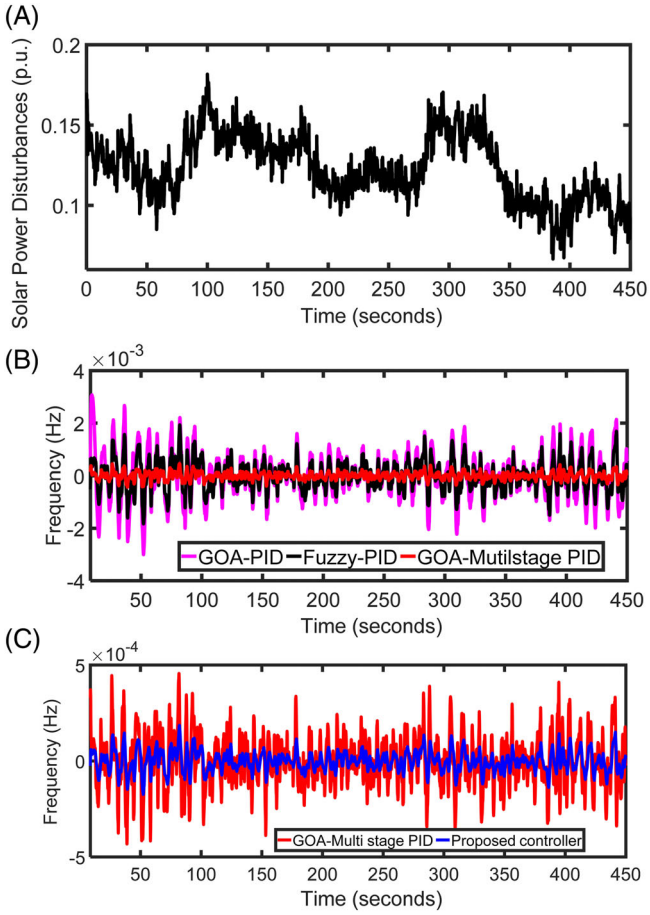

FIGURE 12 A, PV power variations. B, Frequency response of MG (with GOA-PID, Fuzzy-PID, and GOA-multistage PID controllers). C, MG frequency response (with GOA-multistage PID and proposed controllers)

controller reduces the PUS, POS, and ITAE value by 30%, 40%, and 37.26%, respectively, compared to the next best controller.

4.6 | Scenario 6: sensitivity analysis of various controllers against variation in MG internal parameters

In this scenario, besides scenario 5 conditions, the following uncertainties as depicted in Table 9 are considered in the MG LFC performance evaluation. From Figure 15, it can be concluded that the proposed controller exhibits more or less the same performance as scenario 5 conditions.

From Table 10, the proposed controller is less sensitive to multiple disturbances and parametric uncertainties compared to other three controllers. However, GOA-optimized multistage PID controller provides better dynamic response and less sensitive while compared to GOA-PID controller and Fuzzy PID controller.

4.7 | Scenario 7: robustness of the various controllers against ESS uncertainties

In this scenario, the level of robustness of the various controllers are examined through disconnection of various ESSs, viz, FC and BESS from MG at t = 100 seconds. The operating conditions are similar to scenario 5 conditions. Figure 16 depicts the frequency response of MG with various controllers corresponding to ESSs disconnection. As can be seen from Figure 16, the frequency responses of MG, exhibited by the proposed controller, corresponding to ESSs disconnection, are within the range and almost similar to disconnected and normal operation modes. This scenario justifies the robustness of the proposed controller against multi-disturbances and ESS uncertainties of MG.

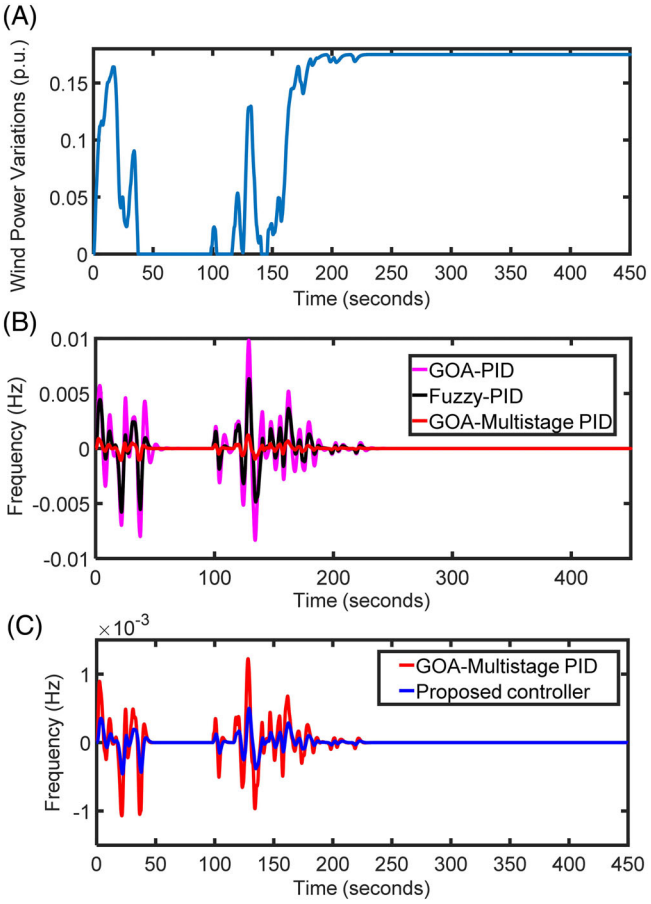

FIGURE 13 A, Wind power variations. B, Frequency response of MG (with GOA-PID, Fuzzy-PID, and GOA-multistage PID controllers)

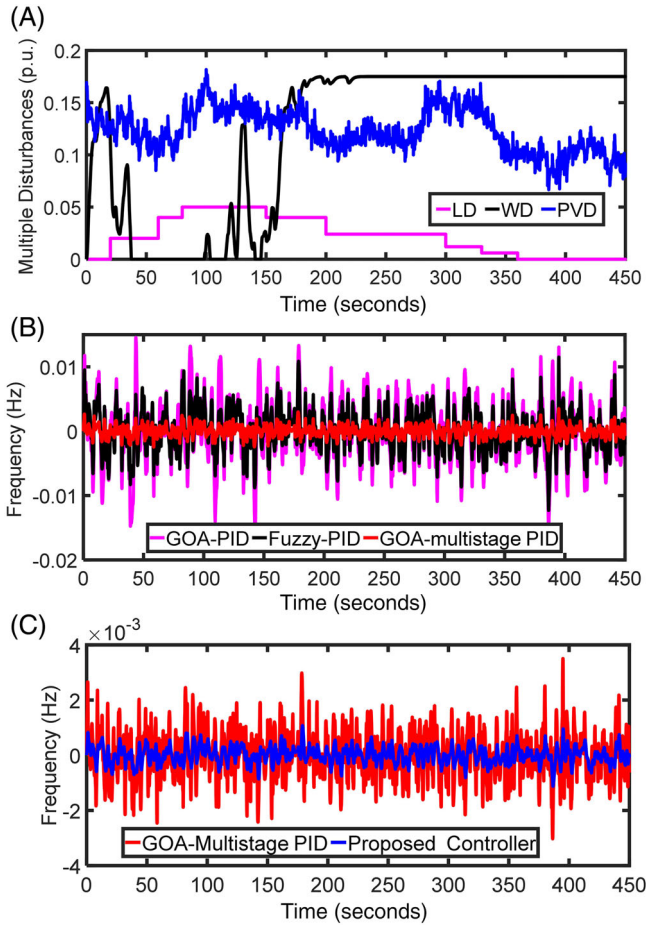

FIGURE 14 A, Multipower disturbances. B, Frequency response of MG (with GOA-PID, Fuzzy-PID, and GOA-multistage PID controllers). C, Frequency response of MG (with GOA-multistage PID and proposed controllers)

Methods	PUS	POS	ITAE
GOA-PID	−0.008	0.01	0.001127
Fuzzy-PID	−0.005	0.006	0.00913
GOA-multistage PID	−0.001	0.001	0.0003091
Proposed controller	−0.0003	0.0004	0.0001152

TABLE 8 Dynamic response analysis of MG with scenario 5 conditions

Parameters	Percentage variation
R	+30
M	−50
D	−50
T_1, T_2	+20
T_3	+30
T_{FC}	+25

TABLE 9 Parametric uncertainties in MG

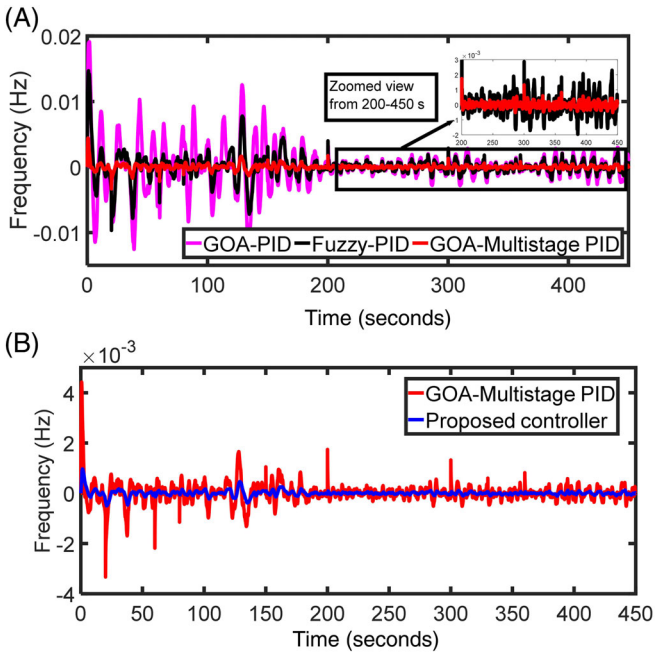

FIGURE 15 A, MG frequency response (with GOA-PID, Fuzzy-PID, and GOA-multistage PID controllers). B, Frequency response of MG (with GOA-multistage PID and proposed controllers)

Methods	PUS	POS	ITAE
GOA-PID	−0.013	0.02	0.0015778
Fuzzy-PID	−0.008	0.014	0.0010823
GOA-multistage PID	−0.0035	0.0042	0.0004216
Proposed controller	−0.00034	0.0007	0.000135492

TABLE 10 Dynamic response analysis of MG with scenario 5 conditions

5 | OBSERVATIONS FROM RESULTS

Diversity in generation/load, functional complexity, change of structure (uncertainty), and variable nature of RES are some key intrinsic characteristics of islanded MG. These characteristics along with ESS uncertainties and load changes introduce large frequency excursions in MG. The GOA and Fuzzy PID controllers are

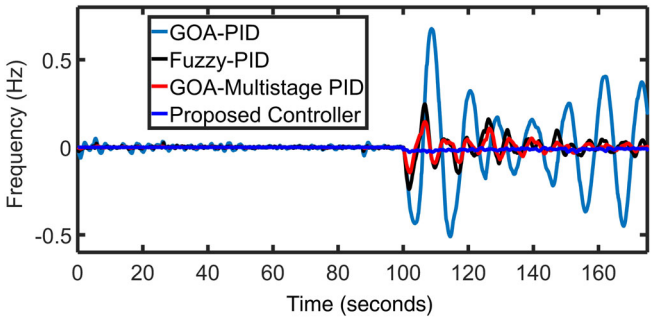

FIGURE 16 Frequency response of MG against ESS uncertainties

underperformed in certain operating scenarios. The GOA optimized multistage PID controller experiences better frequency response against these operating scenarios over the aforementioned controllers. However, the limitations encountered by the GOA multistage PID controller is overcome by the proposed fuzzy tuned multistage PID controller and met the all possible specifications of LFC simultaneously. Moreover, the proposed controller exhibits a better dynamic performance in terms of PUS/POS, settling times, and ITAE value. Furthermore, the proposed controller is robust against RES, MG, and ESS uncertainties. The above characteristics demonstrate that the proposed controller is a suitable option for LFC problems in MG and modern power grids.

6 | CONCLUSION

Fine-tuning of the multistage PID controller to improve the frequency dynamics of an autonomous microgrid has been proposed. The FLA has been applied to generate optimal settings of multistage PID controller. Load perturbations, daily sun irradiations and nature of wind speed variability, ESS, and parametric uncertainties have been considered to show their impact on frequency control. The simulation results and quantitative analysis proved that the proposed controller is promising in dynamic response improvement in terms of fast settling times, less over/undershoots, and low ITAE value. Besides that, the proposed controller is more stubborn to internal MG and ESS uncertainties in addition to RES intermittencies compared to well-established Fuzzy PID, GOA PID, and multistage PID controller, which signify the value of the proposed controller. This study can be further extended by considering communication delays in the LFC analysis, PV, and wind power participation in secondary frequency control by limiting the role of energy storage systems with the aid of the proposed controller.

PEER REVIEW

The peer review history for this article is available at https://publons.com/publon/10.1002/2050-7038.12674.

DATA AVAILABILITY STATEMENT

Data sharing is not applicable to this article as no new data were created or analyzed in this study. All data are available in websites and provided in references.

ORCID

Anil Annamraju https://orcid.org/0000-0003-3368-9628

REFERENCES

1. Dekker J, Nthontho M, Chowdhury S, Chowdhury SP. Economic analysis of PV/diesel hybrid power systems in different climatic zones of South Africa. *Int J Electr Power Energy Syst*. 2012;40(1):104-112.
2. IEEE Std 1547.4 - 2011 - IEEE Guide for Design, Operation, and Integration of Distributed Resource Island Systems with Electric Power Systems: July 20, 2011:1-54.
3. Lee D, Wang L. Small-signal stability analysis of an autonomous hybrid renewable energy power generation/energy storage system part I: time-domain simulations. *IEEE Trans Energy Convers*. 2008;23(1):311-320.

4. Obaid ZA, Cipcigan LM, Abrahim L, Muhssin MT. Frequency control of future power systems: reviewing and evaluating challenges and new control methods. *J Mod Power Syst Clean Energy*. 2019;7(1):9-25.
5. Annamraju A, Nandiraju S, Frequency control in an autonomous two-area hybrid microgrid using grasshopper optimization based robust PID controller. Paper presented at: 2018 8th IEEE India International Conference on Power Electronics (IICPE); December 13-15, 2018; Jaipur, India:1-6.
6. Bevrani H, Feizi MR, Ataee S. Robust frequency control in an islanded microgrid: H_∞ and μ synthesis approaches. *IEEE Trans Smart Grid*. 2016;7(2):706-717.
7. Annamraju A, Nandiraju S. Robust frequency control in an autonomous microgrid: a two-stage adaptive fuzzy approach. *Electr Power Compon Syst*. 2018;46(1):83-94.
8. Alhelou HH, Hamedani-Golshan ME, Zamani R, Heydarian-Forushani E, Siano P. Challenges and opportunities of load frequency control in conventional, modern and future smart power systems: a comprehensive review. *Energies*. 2018;11(10):1–35.
9. Şerban I, Marinescu C. Aggregate load-frequency control of a wind-hydro autonomous microgrid. *Renewable Energy*. 2011;36(12):3345-3354.
10. Yang C, Yao W, Fang J, et al. Dynamic event-triggered robust secondary frequency control for islanded AC microgrid. *Appl Energy*. 2019;242:821-836.
11. Tungadio DH, Bansal RC, Siti MW. Optimal control of active power of two micro-grids interconnected with two AC tie-lines. *Electr. Power Compon Syst.* 2017;45(19):2188-2199.
12. Khalghani MR, Khooban MH, Mahboubi-Moghaddam E, Vafamand N, Goodarzi M. A self-tuning load frequency control strategy for microgrids: human brain emotional learning. *Int J Electr Power Energy Syst*. 2016;75:311-319.
13. Grover H, Ojha J, Verma A, Bhatti TS. Adaptive load frequency control of a grid connected solar PV system. Paper presented at: 2019 IEEE International Conference on Environment and Electrical Engineering and 2019 IEEE Industrial and Commercial Power Systems Europe (EEEIC / I&CPS Europe); June 11-14, 2019; Genova, Italy:1-4.
14. Jeya Veronica A, Kumar NS. Load frequency controller design for microgrid using internal model approach. *Int J Renewable Energy Res*. 2017;7(2):778-786.
15. Pahasa J, Ngamroo I. Coordinated control of wind turbine blade pitch angle and PHEVs using MPCs for load frequency control of microgrid. *IEEE Syst J*. 2016;10(1):97-105.
16. Sedhom BE, El-Saadawi MM, Elhosseini MA, Saeed MA, Abd-Raboh EE. A harmony search-based H-infinity control method for islanded microgrid. *ISA Trans*. 2020;99:252–269.
17. Shashi KP, Soumya R. Frequency regulation in hybrid power systems using particle swarm optimization and linear matrix inequalities based robust controller design. *Int J Electr Power Energy Syst*. 2014;63:887-900.
18. Mi Y, Hao X, Liu Y, et al. Sliding mode load frequency control for multi-area time-delay power system with wind power integration. *IET Gener Transm Distrib*. 2017;11(18):4644-4653.
19. Das DC, Roy AK, Sinha N. GA based frequency controller for solar thermal–diesel–wind hybrid energy generation/energy storage system. *Int J Electr Power Energy Syst*. 2012;43(1):262-279.
20. Srinivasarathnam C, Yammani C, Maheswarapu S. Load frequency control of multi-microgrid system considering renewable energy sources using grey wolf optimization. *Smart Sci*. 2019;7(3):198-217.
21. El-Fergany AA, El-Hameed MA. Efficient frequency controllers for autonomous two-area hybrid microgrid system using social-spider optimiser. *IET Gener Transm Distrib*. 2017;11(3):637-648.
22. Shankar G, Mukherjee V. Load frequency control of an autonomous hybrid power system by quasi oppositional harmony search algorithm. *Int J. Electr. Power Energy Syst.* 2016;78:715-734.
23. Ray PK, Mohanty A. A robust firefly–swarm hybrid optimization for frequency control in wind/PV/FC based microgrid. *Appl Soft Comput*. 2018;85:105823.
24. Shankar R, Kumar A, Raj U, Chatterjee K. Fruit fly algorithm-based automatic generation control of multiarea interconnected power system with FACTS and AC/DC links in deregulated power environment. *Int J. Electr. Energy Syst.* 2019;29:1-25.
25. Annamraju A, Nandiraju S. Coordinated control of conventional power sources and PHEVs using JAYA algorithm optimized PID controller for frequency control of a renewable penetrated power system. *Prot Control Mod Power Syst*. 2019;4:28.
26. Bevrani H, Habibi F, Shokoohi S. ANN-based self-tuning frequency control design for an isolated microgrid. In: Vasant P, ed. *Meta-Heuristics Optimization Algorithms in Engineering, Business, Economics, and Finance*. Hershey, Pennsylvania: IGI Global; 2013:357-385: chap 12.
27. Safari A, Babaei F, Farrokhifar M. A load frequency control using a PSO-based ANN for micro-grids in the presence of electric vehicles. *Int J Ambient Energy*. 2018;40(2):1-13.
28. Khezri R, Golshannavaz S, Shokoohi S, Bevrani H. Fuzzy logic based fine-tuning approach for robust load frequency control in a multi-area power system. *Electr Power Compon Syst*. 2016;44(18):2073-2083.
29. Bevrani H, Habibi F, Babahajyani P, Watanabe M, Mitani Y. Intelligent frequency control in an AC microgrid: online PSO-based fuzzy tuning approach. *IEEE Trans Smart Grid*. 2012;3(4):1935-1944.
30. Khadanga RK, Padhy S, Panda S, Kumar A. Design and analysis of multi-stage PID controller for frequency control in an islanded micro-grid using a novel hybrid whale optimization-pattern search algorithm. *Int J Numer Modell*. 2018;31(5):1–15.
31. Uluski R, Kumar J, Venkata SSM, et al. Microgrid controller design, implementation, and deployment: a journey from conception to implementation at the Philadelphia Navy Yard. *IEEE Power Energy Mag*. 2017;15(4):50-62.

32. Anil A, Srikanth NV. Teaching-learning optimization based adaptive fuzzy logic controller for frequency control in an autonomous microgrid. *Int J Renewable Energy Res*. 2017;7(4):1842-1849.
33. Hu J, Shan Y, Xu Y, Guerrero JM. A coordinated control of hybrid ac/dc microgrids with PV-wind-battery under variable generation and load conditions. *Int J Electr Power Energy Syst*. 2019;104:583-592.
34. El-Fergany A. Electrical characterisation of proton exchange membrane fuel cells stack using grasshopper optimiser. *IET Renewable Power Gener*. 2018;12(1):9-17.
35. Sedghisigarchi K, Feliachi A. Impact of fuel cells on load-frequency control in power distribution systems. *IEEE Trans Energy Convers*. 2006;21(1):250-256.
36. Aziz S, Wang H, Liu Y, Peng J, Jiang H. Variable universe fuzzy logic-based hybrid LFC control with real-time implementation. *IEEE Access*. 2019;7:25535-25546.
37. Zhang S, Mishra Y, Shahidehpour M. Fuzzy-logic based frequency controller for wind farms augmented with energy storage systems. *IEEE Trans Power Syst*. 2016;31(2):1595-1603.
38. Annamraju A, Nandiraju S. Robust frequency control in a renewable penetrated power system: an adaptive fractional order-fuzzy approach. *Prot Control Mod Power Syst*. 2019;4(4):181-195.
39. Hajimiragha AH, Zadeh MRD. Research and development of a microgrid control and monitoring system for the remote community of Bella Coola: challenges, solutions, achievements and lessons learned. Paper presented at: 2013 IEEE International Conference on Smart Energy Grid Engineering (SEGE); August 28-30, 2013; Oshawa, ON:1-6.
40. Saremi S, Mirjalili S, Lewis A. Grasshopper optimisation algorithm: theory and application. *Adv Eng Softw*. 2017;105:30-47.

How to cite this article: Annamraju A, Nandiraju S. A novel fuzzy tuned multistage PID approach for frequency dynamics control in an islanded microgrid. *Int Trans Electr Energ Syst*. 2020;30:e12674. https://doi.org/10.1002/2050-7038.12674

A. APPENDIX

A.1. GOA data

Population size = 100; attractive length scale (l) = 1.5; adaptation factor (c) = [0.0001-4]; attraction factor (f) = 0.5; no of iterations = 50.

A.2. WTG data

TABLE A2 Gamesa Company WTG data

Various specifications of WTG		
Power specifications	**Rotor specifications**	**Generator specifications**
Rated output power: 850 kW	Rated diameter: 22 m	Type: Squirrel cage induction generator
Cut-in wind speed: 4.0 m/s	Swept area: 2124.0 m^2	Voltage: 690 V
Cut-out wind speed: 25.0 m/s	Number of blades: 2	Frequency: 50/60 Hz
Rated wind speed: 16.0 m/s	Tip speed: 90 m/s	Maximum generator output speed: 1900 RPM

A.3. PV data

TABLE A3 Kyocera Company PV module data (KC200GT Model)

Electrical performance at STC:1000 w/m^2 and temperature 25°C	
Rated output power: 200kw	**Open circuit voltage (V_{oc}): 38.6 V**
Maximum power voltage: 26.3 V	Short circuit current (I_{sc}) = 8.21 A
Maximum power current: 7.61 A	Number of cells per module: 54
Maximum system voltage:600 V	